Deciphering the biosynthetic origin of L-*allo*-isoleucine

Qinglian Li, Xiangjing Qin, Jing Liu, Chun Gui, Bo Wang, Jie Li, and Jianhua Ju*

CAS Key Laboratory of Tropical Marine Bio-resources and Ecology, Guangdong Key Laboratory of Marine Materia Medica, RNAM Center for Marine Microbiology, South China Sea Institute of Oceanology, Chinese Academy of Sciences, Guangzhou 510301, China

*Email: jju@scsio.ac.cn

Supporting Information

Table of Contents **Page**

Table S1. Primers used in this study.

Name	Sequence (5'-3')	Purpose
mfnH-DelF	ATCCGTCGCTACTACGAACTAGTGGACGCGGCGGATTAC attccggggatccgtcgacc	For disrupting *mfnH*
mfnH-DelR	CTGATCCGCGAAATAGGTGTACCGACGCCAGATCTTCTC tgtaggctggagctgcttc	
mfnO-DelF	ACCTCGGCGTCTTCGGCCGACCGGCGTCGAGAGGCGCT Cattccggggatccgtcgacc	For disrupting *mfnO*
mfnO-DelR	ATACGAATCGGCTGCCTCGCCGCGGTGTACGGCAGCTAG tgtaggctggagctgcttc	
mfnH-TF	GAGGAATGGTTCACAGCTGCC	For verifying the disruption of *mfnH*
mfnH-TR	TCTCTTCCAGAGCGATGGCGA	
mfnO-TF	ACGACGATCCGATCAGCCGC	For verifying the disruption of *mfnO*
mfnO-TR	CTGTCTGACGGCGCTCCAGT	
dsaD-DelF	GGAGTCGGGCAGTTCGCCGCGCTGGATGCCGAACAGCGC ACTAGTattccggggatccgtcgacc (*Spe*I site underlined)	For disrupting *dsaD*
dsaD-DelR	ACGGAGCGCTGCGCCGCCCCCGCCTTCGGCACCGCGTTC ACTAGTtgtaggctggagctgcttc (*Spe*I site underlined)	
dsaE-DelF	CAGTGGGGCGAAGAAGTACGTGTCACGCCGACTGAACCG ACTAGTattccggggatccgtcgacc (*Spe*I site underlined)	For disrupting *dsaE*
dsaE-DelR	GAGAGCTCTCCCACCGAGGTCAATGAGGCCCGGGTGCGT ACTAGTtgtaggctggagctgcttc (*Spe*I site underlined)	
dsaD-TF	GCTGTGACGCGACGAGTT	For verifying the disruption of *dsaD*
dsaD-TR	GGCCGGAGTGCATATCG	
dsaE-TF	TCCTGTGGCGGTTCGTG	For verifying the disruption of *dsaE*
dsaE-TR	ACAGCCCGTACACACCG	
dsaD-exp-F	TATCATATGGTGCATATCGTGACCAC (*Nde*I site underlined)	For cloning and expression of *dsaD*
dsaD-exp-R	TATGAATTCTCATGTGATCGCCGAC (*Eco*RI site underlined)	
dsaE-exp-F	TATCATATGATGACCGAGAGCTCTC (*Nde*I site underlined)	For cloning and expression of *dsaE*
dsaE-exp-R	TATGAATTCTCACACCAGTGGGGCG (*Eco*RI site underlined)	
mfnO-exp-F	AAATTTCCCATATGACCACGACCTCATCCG (*Nde*I site underlined)	For cloning and expression of *mfnO*
mfnO-exp-R	ATATGAATTCTCAGGCCTCGTGGTTCAC (*Eco*RI site underlined)	
mfnH-exp-F	AAATTTCCCATATGGGGCGCTCCGAGACC (*Nde*I site underlined)	For cloning and expression of *mfnH*
mfnH-exp-R	ATATGAATTCCTACACCGACTGATCCGC (*Eco*RI site underlined)	
EcBCAT-exp-F	GATAGGGCGCTAGCATGACCACGAAGAAAGCT (*Nhe*I site underlined)	For cloning and expression of EcBCAT
EcBCAT-exp-R	CATCGAATTCTTATTATTGATTAACTTGATCTA (*Eco*RI site underlined)	
MsBCAT-exp-F	GATAGGGCGCTAGCATGAATAGCGGTCCGCT (*Nhe*I site underlined)	For cloning and expression of MsBCAT
MsBCAT-exp-R	CATCGAATTCTTACTAGTTCAGCCGGGCCATCCA (*Eco*RI site underlined)	

DsaD-K198L-F	GGCACCGGAGCCGCCCTGTGCGCGGGCAA	For construction of DsaD/K198L mutant
DsaD-K198L-R	AGGGCGGCTCCGGTGCCGCCGGCGGCG	
MfnO-K206L-F	GGCACGGGGGCGGCCCTGTGCGGTGGCAA	For construction of MfnO/K206L mutant
MfnO-K206L-R	AGGGCCGCCCCCGTGCCGCCCGGAGCGG	
MfnH-Y10F-F	ACCATCCGTCGCTTTTACGAACTAG	For construction of MfnH/Y10F mutant
MfnH-Y10F-R	GTAGCGACGGATGGTCTCGGAGCGC	
MfnH-Y11F-F	ATCCGTCGCTACTTTGAACTAGTGG	For construction of MfnH/Y11F mutant
MfnH-Y11F-R	AAAGTAGCGACGGATGGTCTCGGAG	
MfnH-D15L-F	TACGAACTAGTG CTG GCGGCGGATT	For construction of MfnH/D15L mutant
MfnH-D15L-R	CAGCACTAGTTCGTAGTAGCGACGG	
MfnH-F26A-F	ATGTTCCGTATA GCG TGCGACGACC	For construction of MfnH/F26A mutant
MfnH-F26A-R	CGCTATACGGAACATGGCCTCGTAA	
MfnH-Y32F-F	GACGACCTGATATTTGAGCGGGCCG	For construction of MfnH/Y32F mutant
MfnH-Y32F-R	AAATATCAGGTCGTCGCAGAATATA	
MfnH-R34L-F	CTGATATACGAGCTGGCCGGAACCG	For construction of MfnH/R34L mutant
MfnH-R34L-R	AGCTCGTATATCAGGTCGTCGCAG	
MfnH-F49A-F	GAGTTCCGTCACGCGTATCTCGCCG	For construction of MfnH/F49A mutant
MfnH-F49A-R	CGCGTGACGGAACTCCACGATTCCC	
MfnH-Y50F-F	TTCCGTCACTTCTTTCTCGCCGACC	For construction of MfnH/Y50F mutant
MfnH-Y50F-R	AAGAAGTGACGGAACTCCACGATT	
MfnH-R54L-F	TATCTCGCCGACCTGAAGATCAGGT	For construction of MfnH/R54L mutant
MfnH-R54L-R	CAGGTCGGCGAGATAGAAGTGACGG	
MfnH-H61F-F	AGGTCGGGACGGTTTTCTCTGGACG	For construction of MfnH/H61F mutant
MfnH-H61F-R	AAACCGTCCCGACCTGATCTTGCGG	
MfnH-F79A-F	GCCAGAGGAGTCGCGACCGGACAAC	For construction of MfnH/F79A mutant
MfnH-F79A-R	CGCGACTCCTCTGGCGGCGACCCAG	
MfnH-D95L-F	ACCCGGTGGGCCCTGTTCCACCAGT	For construction of MfnH/D95L mutant
MfnH-D95L-R	CAGGGCCCACCGGGTGGTCACGGCT	
MfnH-R107L-F	AAGATCTGGCGTCTGTACACCTATT	For construction of MfnH/R107L mutant
MfnH-R107L-R	AGACGCCAGATCTTCTCTCCCCGG	
DsaE-D22L-F	CCGGTTGGTGCTCGCGGACGACGTC	For construction of

DsaE-D22L-R	AGCACCAACCGGTAGTACTCACGCAC	DsaE/D22L mutant
DsaE-D102L-F	GCCTGGAATTCGCCCTCTTCTTTCTGC	For construction of DsaE/D102L mutant
DsaE-D102L-R	AGGGCGAATTCCAGGCGGACTTGGCG	
DsaE-H68F-F	GATCGAGAGCGGTCGGTTTACCGTCGCCACGGTCG	For construction of DsaE/H68F mutant
DsaE-H68F-R	CGACCGTGGCGACGGTAAACCGACCGCTCTCGATC	

Table S2. ^{1}H and ^{13}C NMR spectroscopic data for compound 7 in CD_3OD.

Position	**7**	**7**
	δ_H, mult. (*J* in Hz)	δ_C
NMeVal		
α	5.01,d (11.6)	64.0
β	2.34, m	26.4
ϒ$_A$-Me	0.90,d (6.4)	19.8
ϒ$_B$-Me	1.11, d (6.4)	20.4,
NMe	3.07, s	30.5
C=O		169.4
Leu		
α	5.04, d (7.3)	51.1
β	2.02, m; 1.48, m	41.2
ϒ	1.99, m	26.3
δ$_A$-Me	0.94, d (6.4)	24.0
δ$_B$-Me	1.03, d (6.4)	20.0
C=O		175.7
Pip		
α	5.08, m	50.3
β	2.77, d (15.5); 1.94, m	32.1
ϒ	3.80, br s	62.1
δ	2.97, br s	54.2
C=O		171.7
D-allo-ile		
α	5.30, d (10.2)	56.6
β	1.87, m	36.6
β-Me	1.10, d (6.1)	16.5
ϒ	1.49, m; 1.24, m	27.3
δ-Me	0.98, t (5.3)	12.2
C=O		177.7
Tyr-OMe		
α	5.10, m	54.3
β	3.51, dd (14.1, 4.4)	38.3
1	3.17, m	131.5
2,6	7.31, d (8.5)	131.7
3,5	6.77, d (8..5)	114.9
4		160.1
4-OMe	3.71, s	55.8
C=O		174.8
Thr		
α	4.32, d (3.7)	56.5
β	4.85, m	70.3
ϒ-Me	0.41, d (6.4)	13.7
C=O		167.9
Val		
α	4.37, t (5.0)	58.5
β	2.05, m	31.8
ϒ$_A$-Me	0.97, d (6.4)	19.0
ϒ$_B$-Me	0.87, d (6.4)	18.3
HC=O	8.12, s	164.0
C=O		172.5

Table S3. Crystal data and structure refinement for compound 7. (03162A)

Identification code	03162A	
Empirical formula	C86 H162 N16 O35	
Formula weight	1980.31	
Temperature	150(2) K	
Wavelength	1.54184 Å	
Crystal system	Orthorhombic	
Space group	$P2_12_12$	
Unit cell dimensions	a = 24.9455(2) Å	α= 90°.
	b = 19.28742(18) Å	β= 90°.
	c = 11.27639(9) Å	γ = 90°.
Volume	5425.46(9) $Å^3$	
Z	2	
Density (calculated)	1.212 Mg/m^3	
Absorption coefficient	0.783 mm^{-1}	
F(000)	2140	
Crystal size	0.420 x 0.390 x 0.340 mm^3	
Theta range for data collection	2.896 to 67.037°.	
Index ranges	-29<=h<=29, -23<=k<=20, -13<=l<=13	
Reflections collected	47323	
Independent reflections	9610 [R(int) = 0.0319]	
Completeness to theta = 67.037°	99.6 %	
Absorption correction	Semi-empirical from equivalents	
Max. and min. transmission	1.00000 and 0.71465	
Refinement method	Full-matrix least-squares on F^2	
Data / restraints / parameters	9610 / 0 / 635	
Goodness-of-fit on F^2	1.054	
Final R indices [I>2sigma(I)]	R1 = 0.0457, wR2 = 0.1275	
R indices (all data)	R1 = 0.0472, wR2 = 0.1293	
Absolute structure parameter	-0.03(4)	
Extinction coefficient	n/a	
Largest diff. peak and hole	1.156 and -0.388 $e.Å^{-3}$	

Crystallographic data (including structure factors) for compound **7** have been deposited in the Cambridge Crystallographic Data Center with an acquisition number 1432080. Copies of the data can be obtained, free of charge, on application to CCDC, 12 Union Road, CB2 1EZ, UK [fax: +44-0-1223-336033 or e-mail: deposit@ccdc.cam.ac.uk].

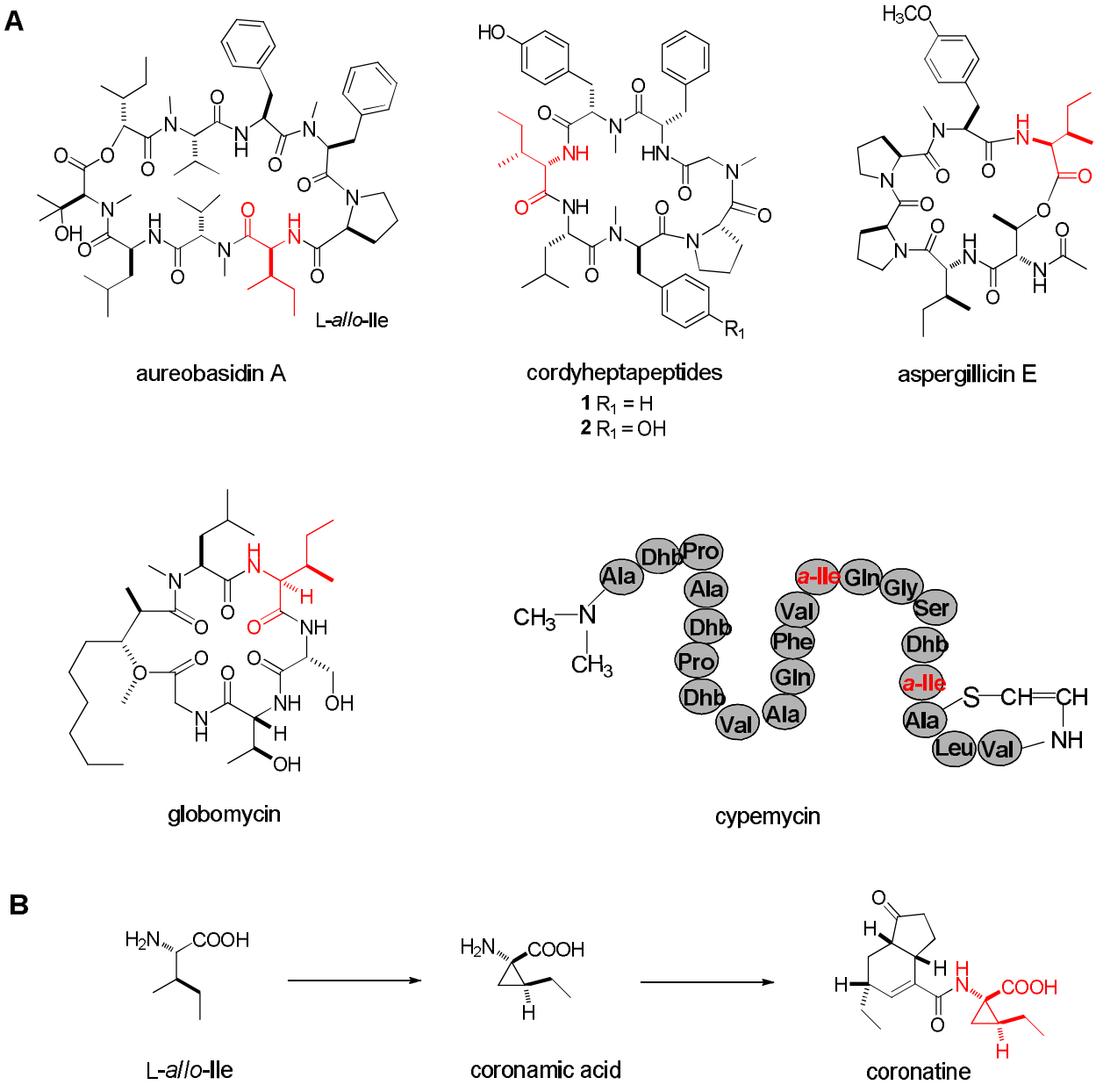

Figure S1. (A) Selected natural products containing the L-*allo*-Ile moiety (colored red). (B) L-*allo*-Ile is used as a precursor to synthesize phytotoxin coronatine.

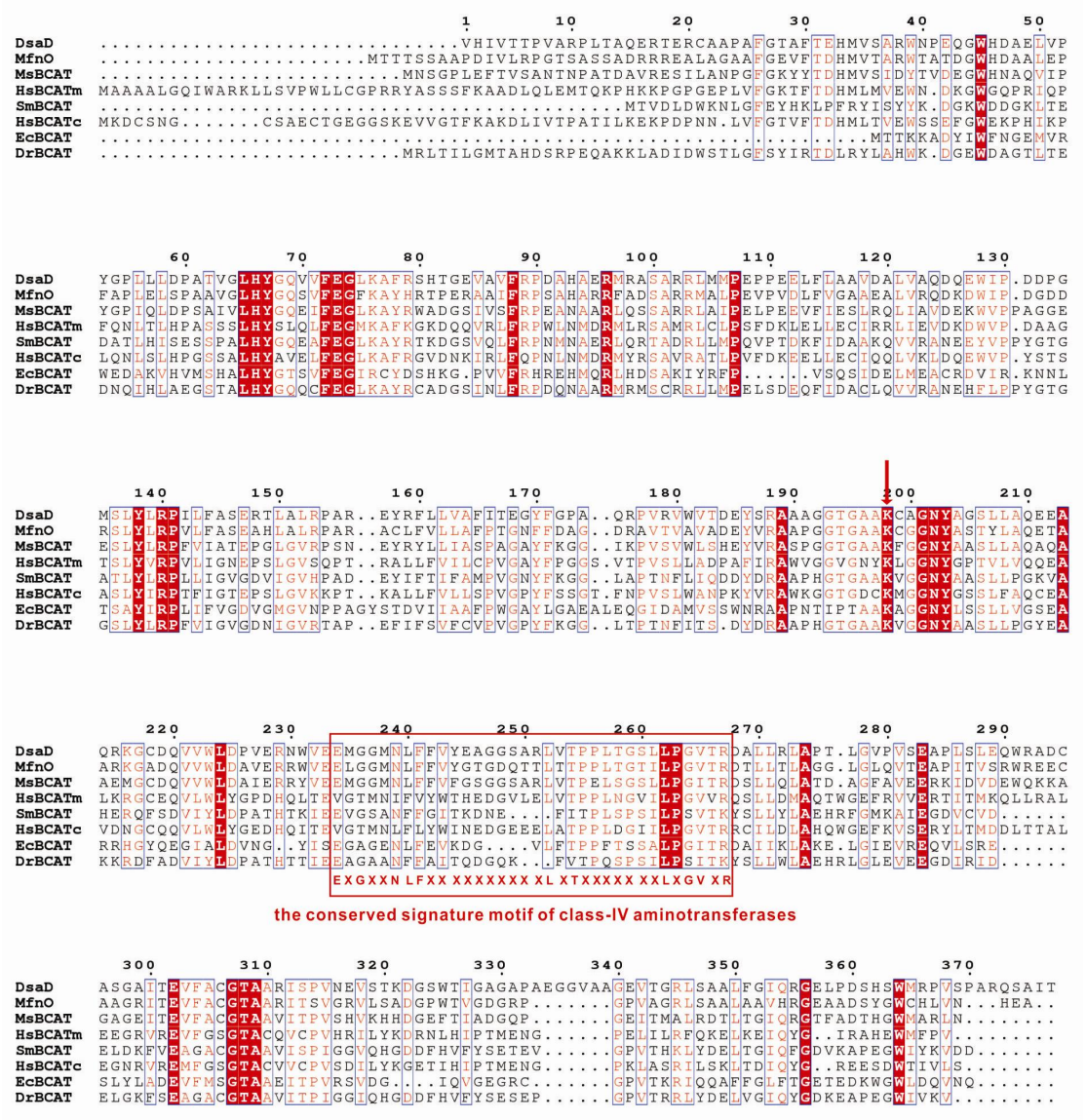

Figure S2. Sequence alignments of DsaD/MfnO with the branched-chain aminotransferases (BCATs) from *Mycobacterium smegmatis* (MsBCAT, NCBI gi number: 399233140), human mitochondrial (hsBCATm, NCBI gi number: 13786631), *Streptococcus mutans* (SmBCAT, NCBI gi number: 436408788), human cytosolic (hsBCATc, NCBI gi number: 75766442), *E.coli* (EcBCAT, NCBI gi number: 30749295), and *Deinococcus radiodurans* (DrBCAT, NCBI gi number: 429544222). The conserved EXGXXNLFX$_n$LXTX$_n$LXGVXR signature motif is indicated by the red box. The PLP binding active-site lysine is indicated with a vertical arrow.

Figure S3A. Alignment of amino acid sequences of DsaE/MfnH and their homologous proteins with delta[5]-3-ketosteroid isomerase from *Comamonas testosteroni* (KSI_{ct}). The following

proteins (with GeneBank IDs) were used for amino acid alignment: WP_030868916.1 from *Streptomyces* sp. NRRL F-2747; WP_013496225.1 from *Thermaerobacter marianensis*; WP_014051297.1 from *Halophilic archaeon* DL31; WP_009886289.1 from *Ferroplasma acidarmanus*; WP_021786773.1 from *Ferroplasma* sp. Type II; WP_029211959.1 from *Arsenicicoccus bolidensis*; WP_006946988.1 from *Dermacoccus* sp. Ellin185; WP_038566685.1 from *Dermacoccus nishinomiyaensis*; WP_035303624.1 from *Actinokineospora inagensis*. The amino acids in DsaE/MfnH and their homologous proteins corresponding to the three catalytic amino acids of KSI_{ct} (Tyr14, Asp38 and Asp99) are shaded in gray.

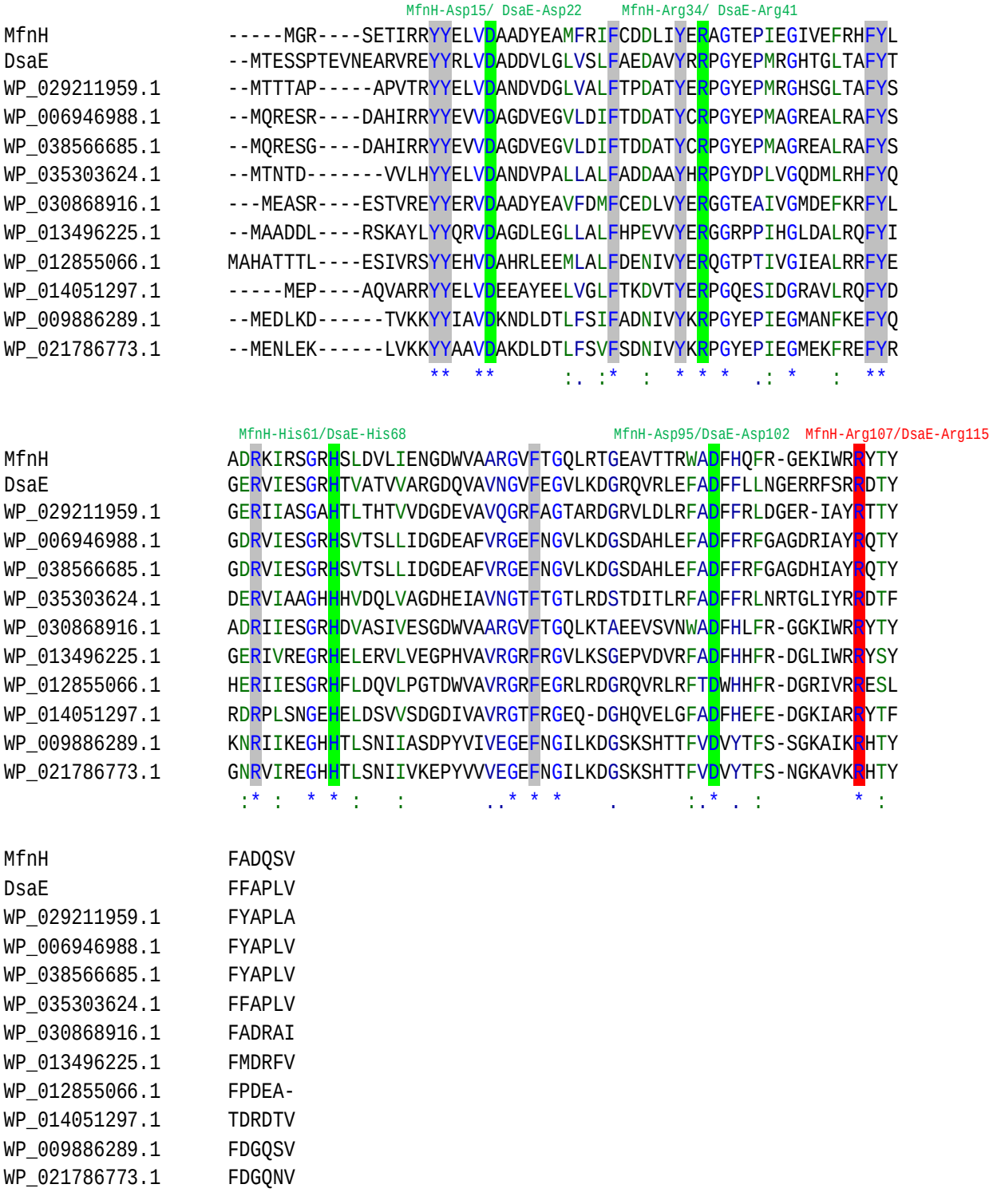

Figure S3B. Alignment of amino acid sequences of DsaE/MfnH with their homologous proteins of unknown function by Clustal W (1.81). Ten hits of the BLAST search of MfnH from the NCBI

database were aligned: WP_029211959.1 from *Arsenicicoccus bolidensis*; WP_006946988.1 from *Dermacoccus* sp. Ellin185; WP_038566685.1 from *Dermacoccus nishinomiyaensis*; WP_035303624.1 from *Actinokineospora inagensis*; WP_030868916.1 from *Streptomyces* sp. NRRL F-2747; WP_013496225.1 from *Thermaerobacter marianensis*; WP_012855066.1 from *Thermomonospora curvata*; WP_014051297.1 from *Halophilic archaeon* DL31; WP_009886289.1 from *Ferroplasma acidarmanus*; WP_021786773.1 from *Ferroplasma* sp. Type II. The fully conserved residues in DsaE/MfnH and their homologues are indicated by blue asterisks. The eight conserved polar amino acids of DsaE/MfnH were demonstrated to have no effect on the enzymatic activity as determined by mutagenesis studies; these are shaded in gray. The four conserved polar amino acids of DsaE/MfnH whose mutation was found to sharply diminish enzymatic activity are shaded in green; and the catalytic arginine residues of DsaE/MfnH are shaded in red.

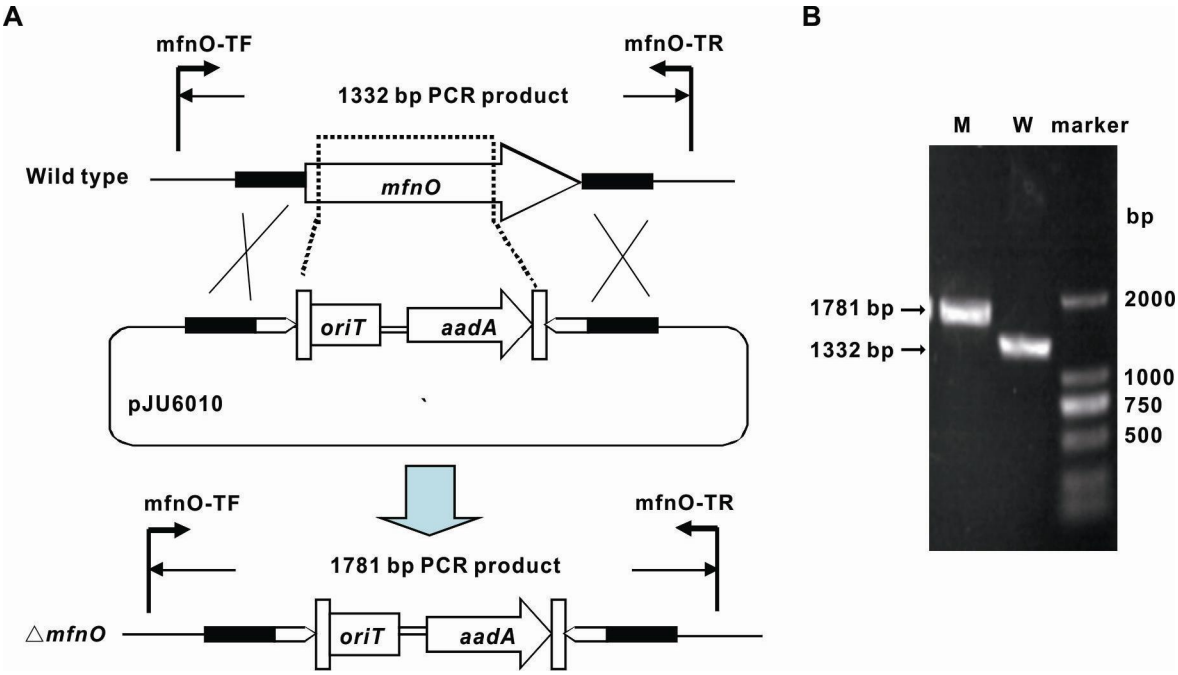

Figure S4. Disruption of *mfnO* in wild-type *S. drozdowiczii* SCSIO 10141 via PCR-targeting. (A) Schematic representation for disruption of *mfnO.* (B*)* PCR analyses of the wild-type strain and the *mfnO* double-cross mutant carried out using the primers listed in Table S1. Marker: DNA molecular ladder; W: using the genomic DNA of *S.drozdowiczii* SCSIO 10141 as template; M: using the genomic DNA of *mfnO* mutant as template.

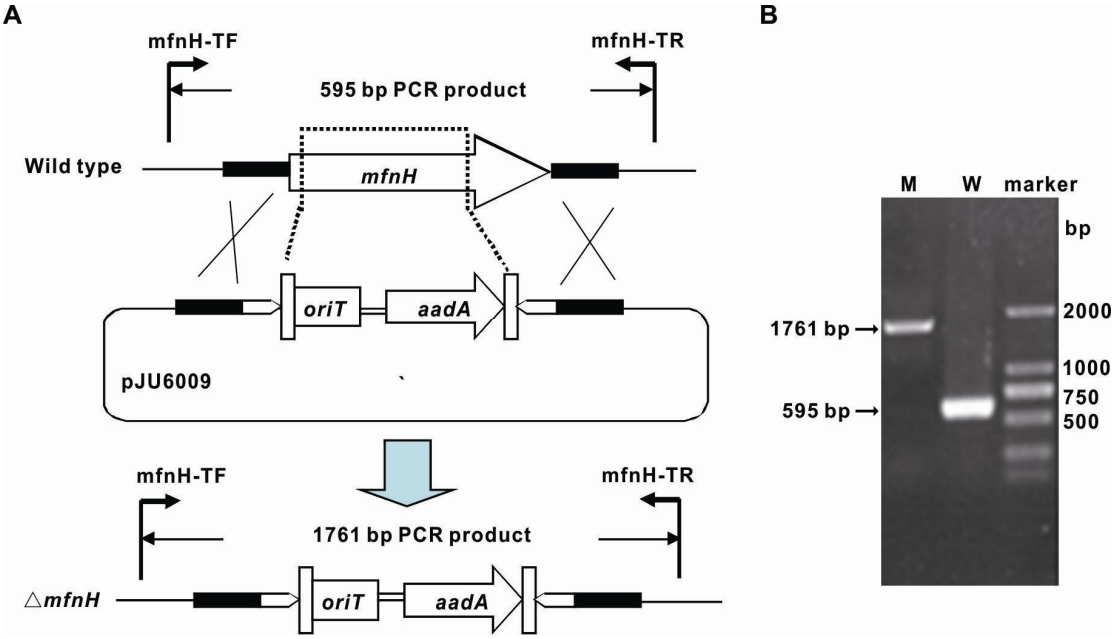

Figure S5. Disruption of *mfnH* in wild-type *S. drozdowiczii* SCSIO 10141 via PCR-targeting. (A) Schematic representation for disruption of *mfnH*. (B) PCR analyses of the wild-type strain and the *mfnH* double-cross mutant carried out using the primers listed in Table S1. Marker: DNA molecular ladder; W: using the genomic DNA of *S. drozdowiczii* SCSIO 10141 as template; M: using the genomic DNA of *mfnH* mutant as template.

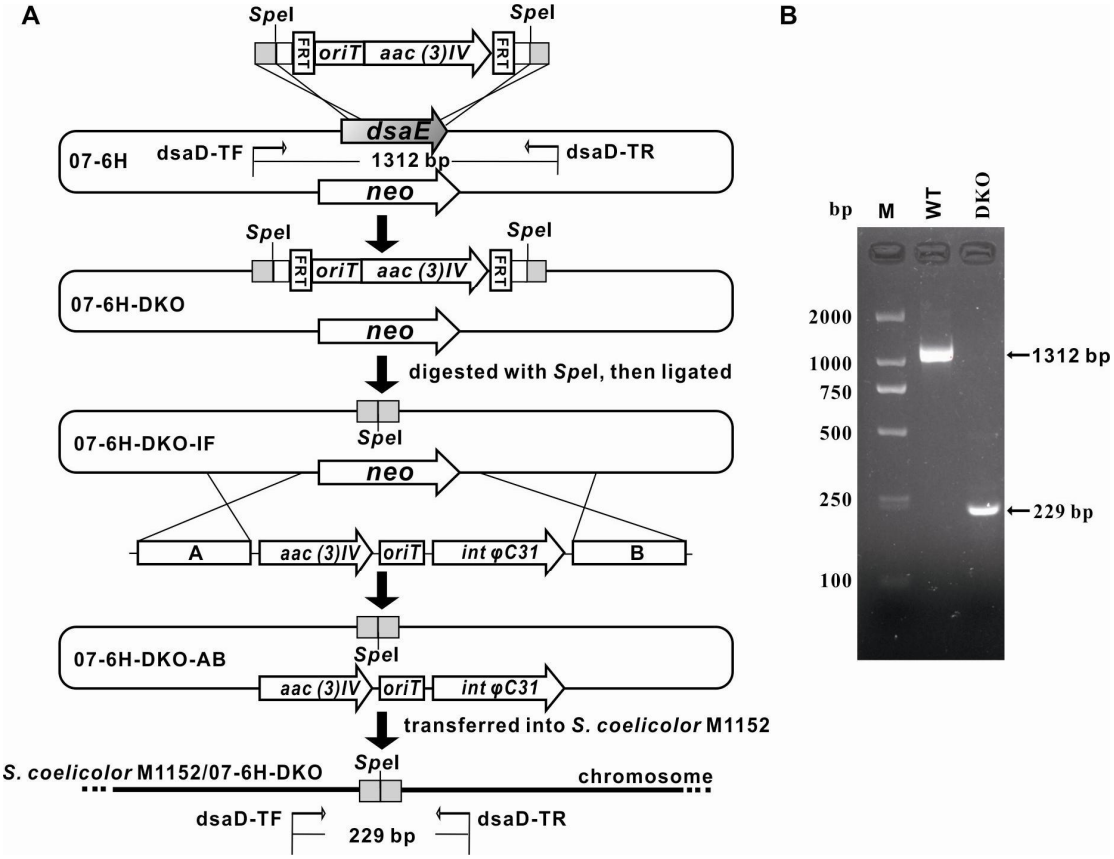

Figure S6. In-frame disruption of *dsaD* within the DSA gene cluster and subsequent heterologous expression in *S. coelicolor* M1152. (A*)* Schematic representation for disruption of *dsaD.* (B*)* PCR analysis of *S. coelicolor* M1152/07-6H-DKO carried out using the primers listed in Table S1. M: DNA molecular ladder; WT: using cosmid 07-6H as template; DKO: using the genomic DNA of *S. coelicolor* M1152/7-6H-DKO as template.

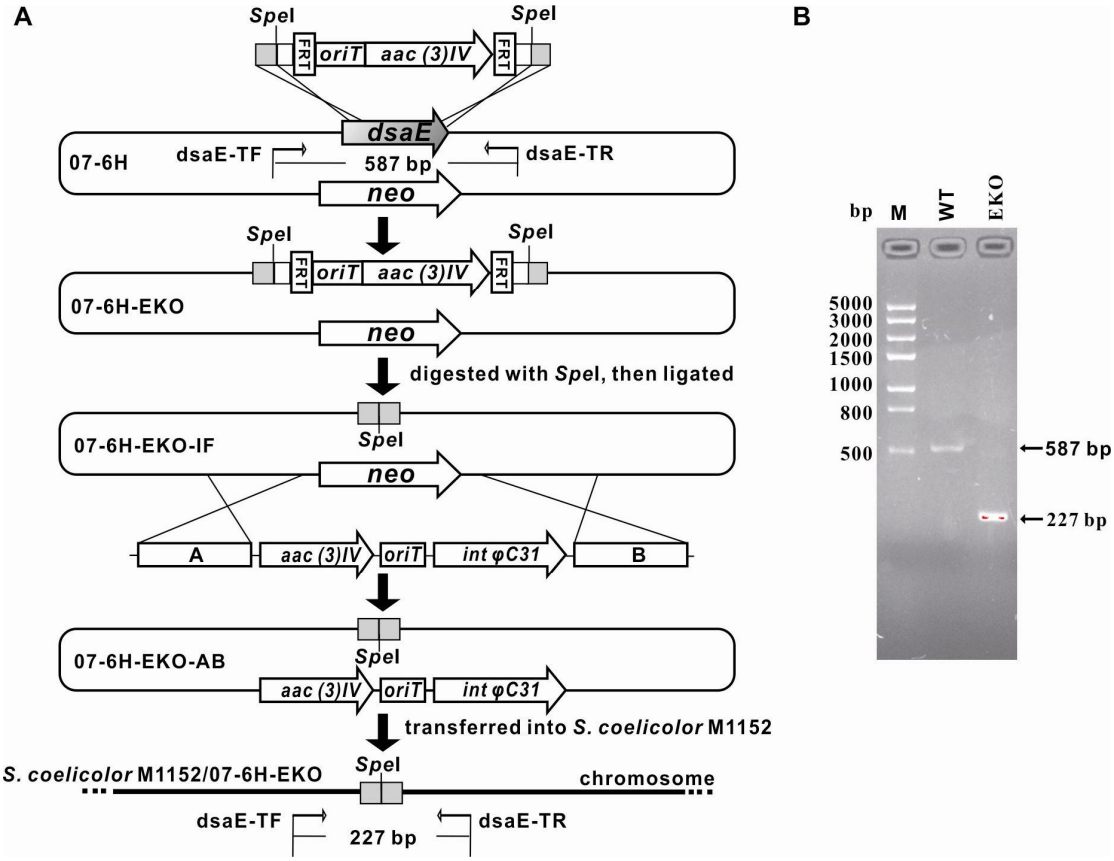

Figure S7. In-frame disruption of *dsaE* within the DSA gene cluster and subsequent heterologous expression in *S. coelicolor* M1152. (A) Schematic representation for disruption of *dsaE.* (B) PCR analysis of *S. coelicolor* M1152/07-6H-EKO carried out using the primers listed in Table S1. M: DNA molecular ladder; WT: using cosmid 07-6H as template; EKO: using the genomic DNA of *S. coelicolor* M1152/7-6H-EKO as template.

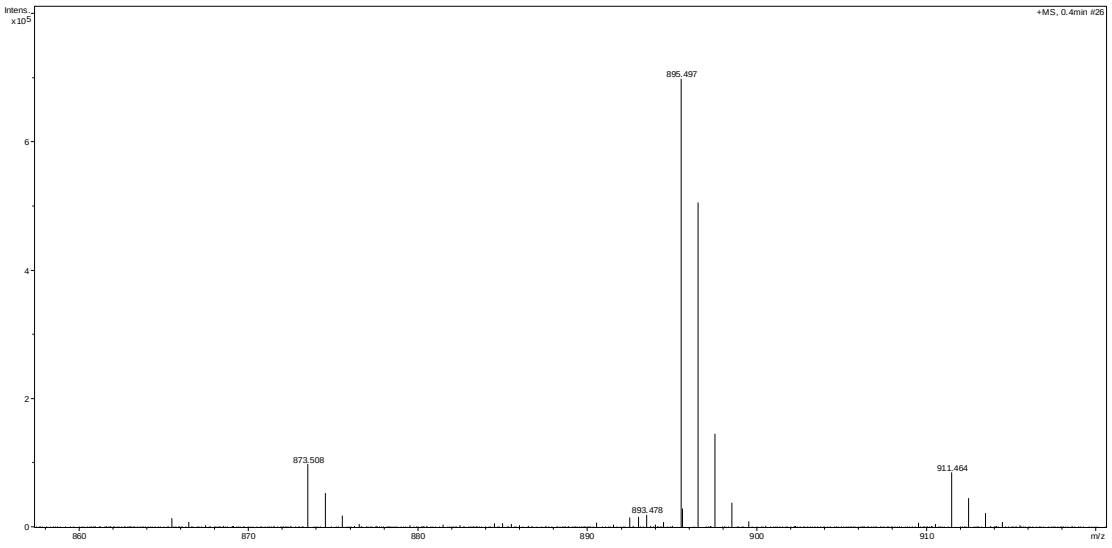

Figure S8. HRESIMS spectrum of compound **7**.

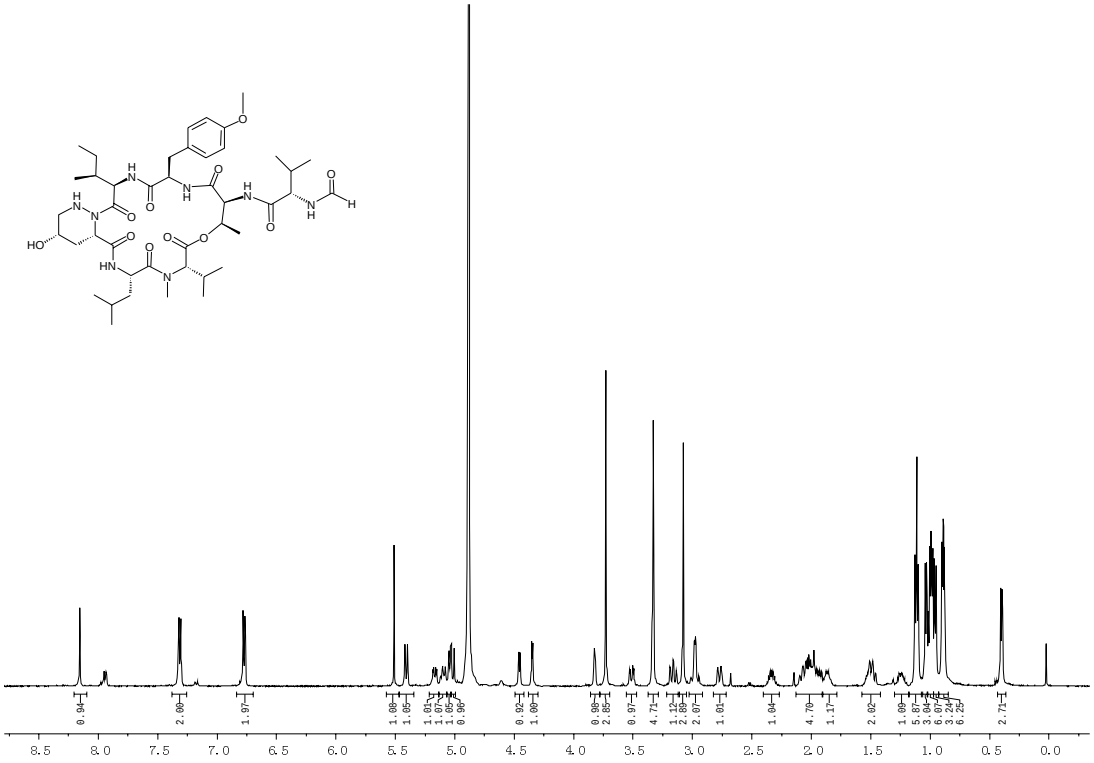

Figure S9. ^{1}H (500 MHz) NMR spectrum of compound **7** in MeOD.

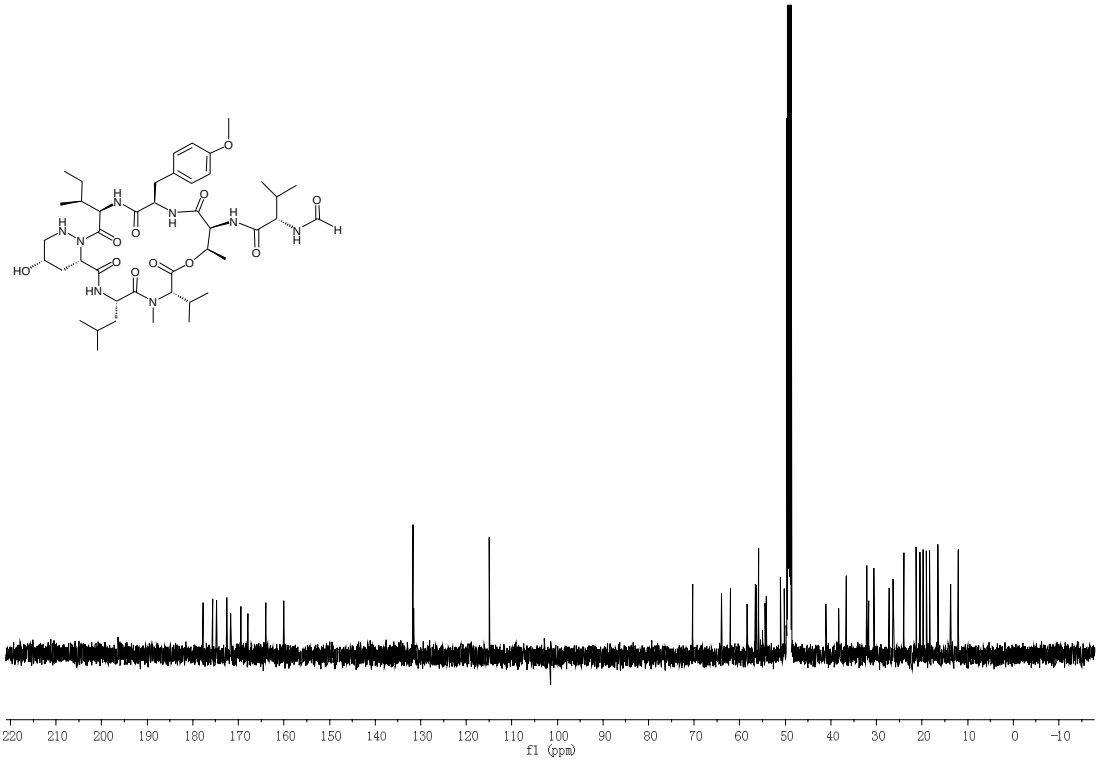

Figure S10. ^{13}C (500 MHz) NMR spectrum of compound **7** in MeOD.

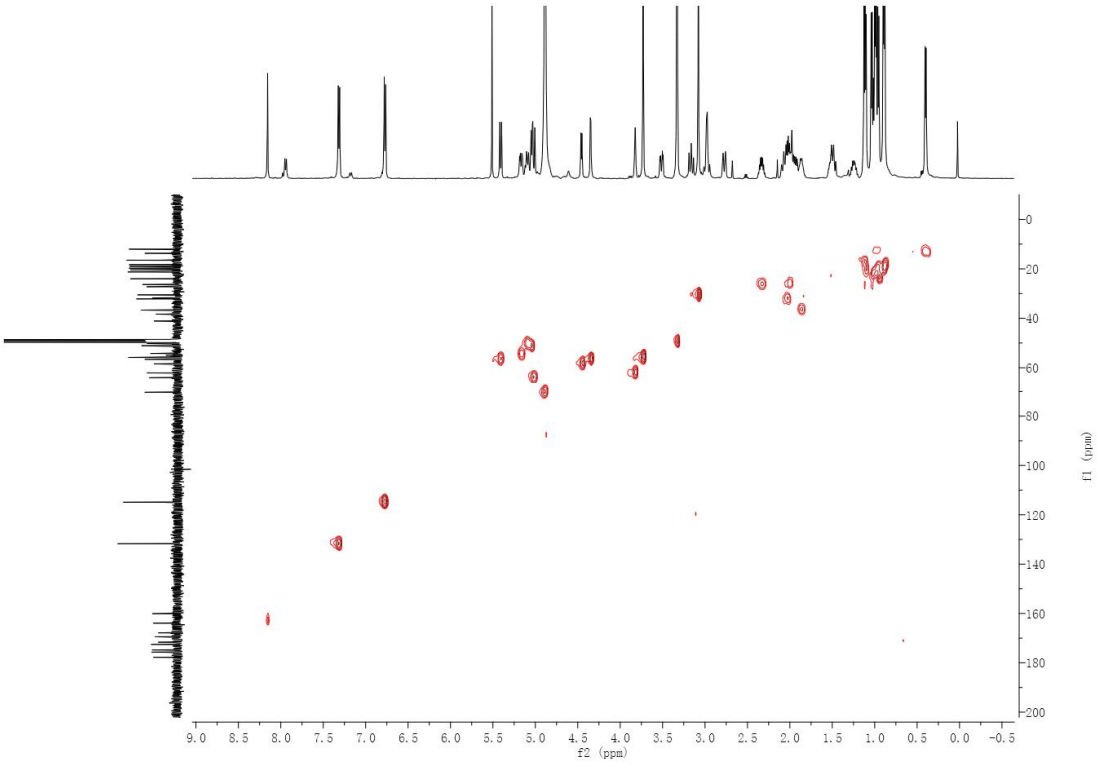

Figure S11. HSQC NMR spectrum of compound **7** in MeOD.

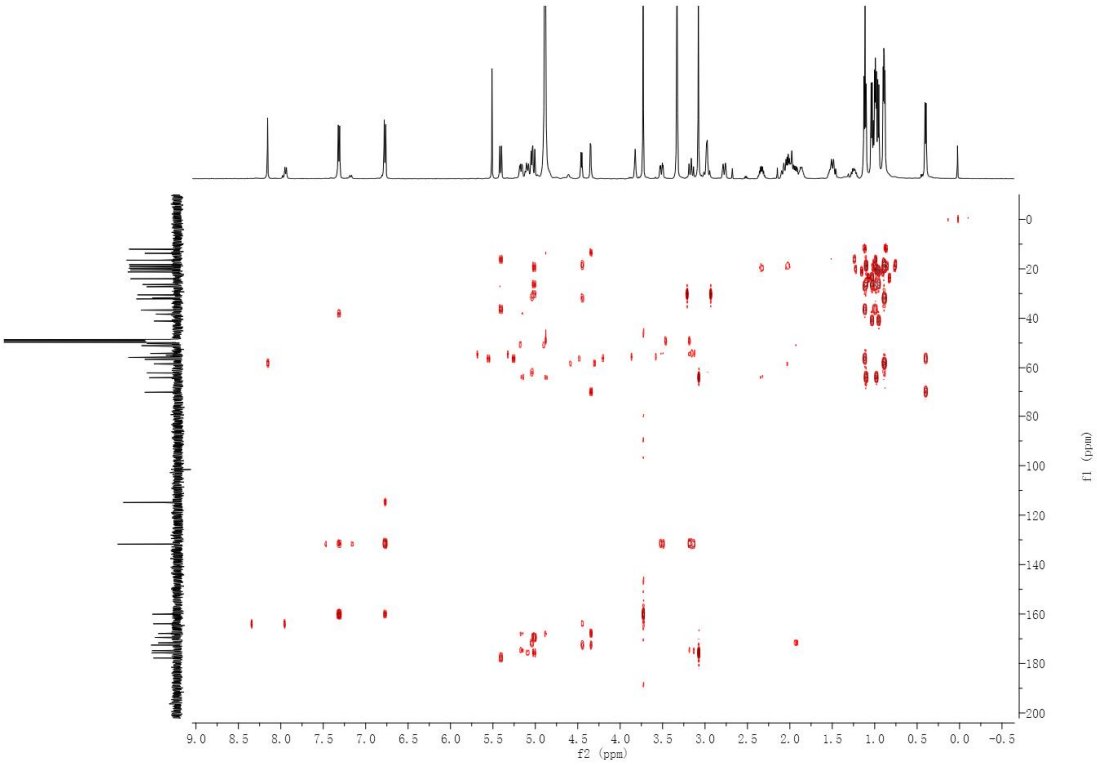

Figure S12. HMBC NMR spectrum of compound **7** in MeOD.

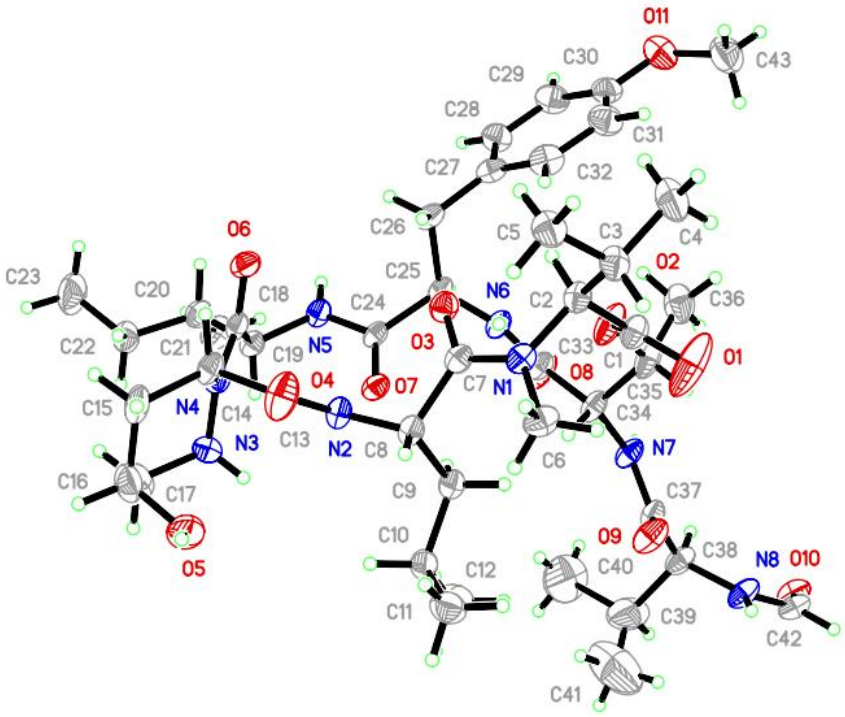

Figure S13. Perspective view of the X-ray structure of **7**.

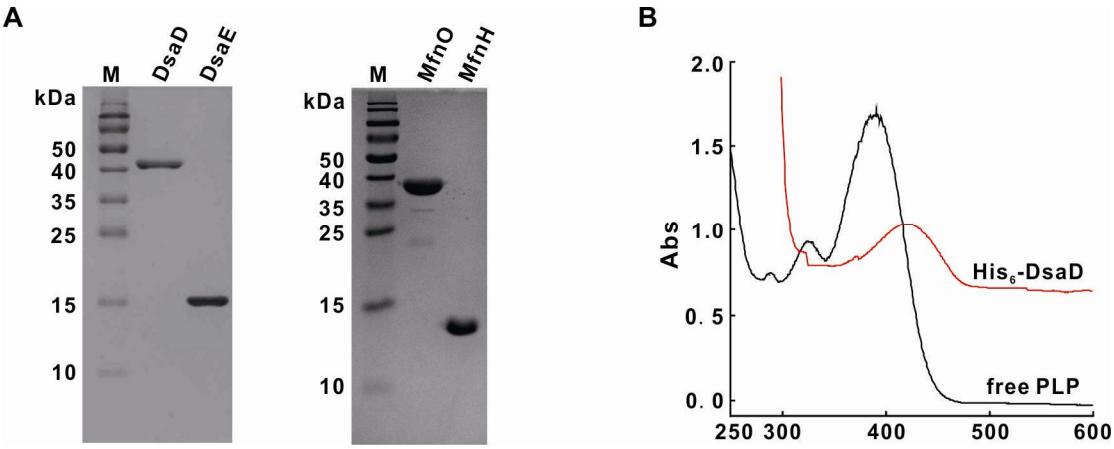

Figure S14. (A) SDS-PAGE analyses of purified His_6-DsaD, His_6-DsaE, His_6-MfnO and His_6-MfnH. (B) UV spectra of His_6-DsaD indicate the presence of PLP covalently linked to the catalytic lysine residue of DsaD via a Schiff base linkage.

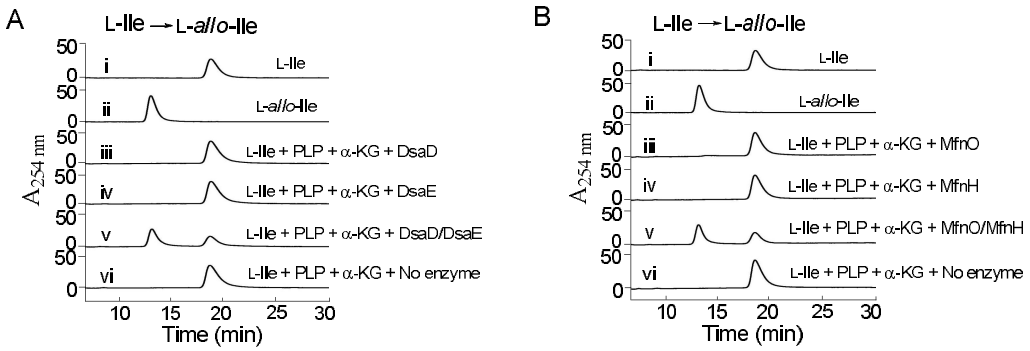

Figure S15. *In vitro* characterization of DsaD/DsaE and MfnO/MfnH in the presence of possible cofactors PLP and α-KG. (A) Production of L-*allo*-Ile proceeds only upon co-incubation of L-Ile with DsaD and DsaE in the presence of possible cofactors PLP and α-KG (v). Enzyme assays with DsaD alone (iii), DsaE alone (iv), or control lacking DsaD/DsaE (vi) gave only the starting substrate L-Ile. (B) Production of L-*allo*-Ile proceeds only upon co-incubation of L-Ile with MfnO and MfnH in the presence of possible cofactors PLP and α-KG (v). Enzyme assays with MfnO alone (iii), MfnH alone (iv), or control lacking MfnO/MfnH (vi) gave only the starting substrate L-Ile.

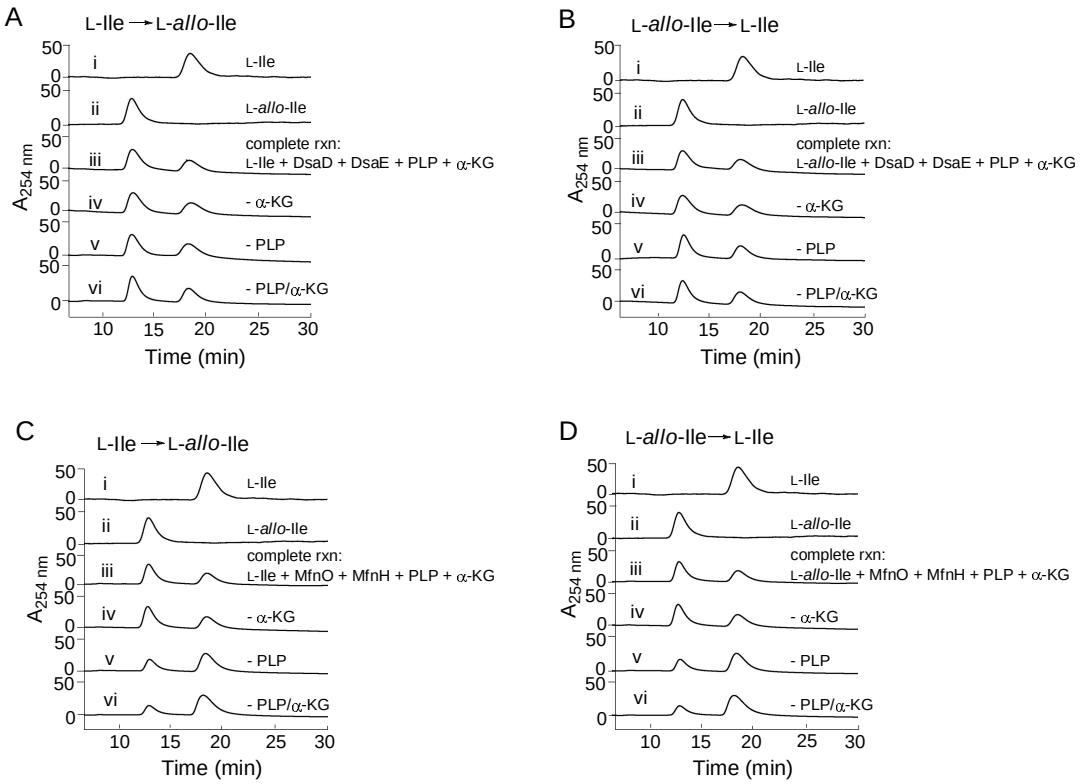

Figure S16. Determination of possible requirement of exogenous PLP and α-ketoglutarate (α-kG) for the DsaD/DsaE or MfnO/MfnH-catalyzed interconversion between L-Ile and L-*allo*-Ile. (A) Removal of exogenous PLP (v), α-KG (iv) and PLP/ α-KG (vi) from the complete reaction containing L-Ile, DsaD/DsaE, PLP and α-KG has no effect on production of L-*allo*-Ile. (B) Removal of exogenous PLP (v), α-KG (iv) and PLP/ α-KG (vi) from the complete reaction containing L-*allo*-Ile, DsaD/DsaE, PLP and α-KG has no effect on production of L-Ile. (C) Removal of exogenous PLP (v), α-KG (iv) and PLP/ α-KG (vi) from the complete reaction containing L-Ile, MfnO/MfnH, PLP and α-KG has no effect on production of L-*allo*-Ile. (D) Removal of exogenous PLP (v), α-KG (iv) and PLP/ α-KG (vi) from the complete reaction containing L-*allo*-Ile, MfnO/MfnH, PLP and α-KG has no effect on production of L-Ile.

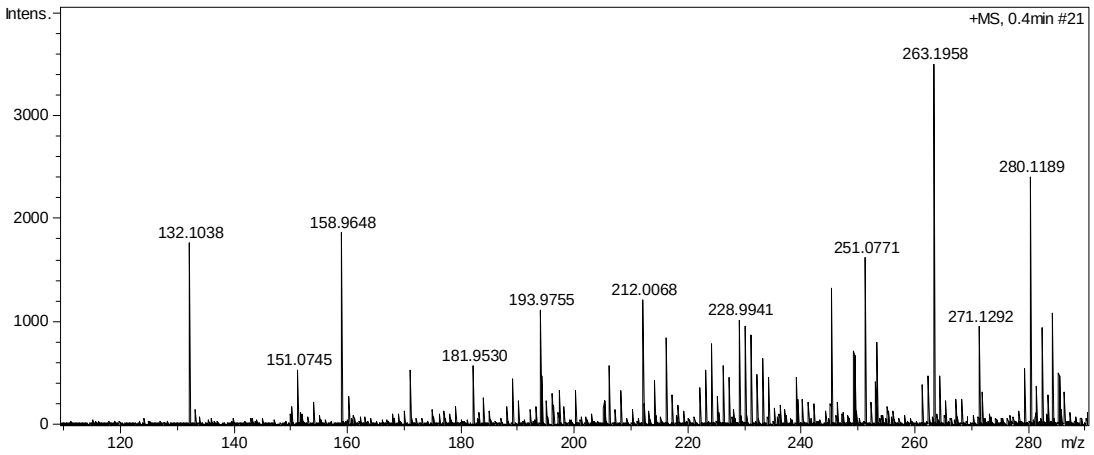

Figure S17. HRESIMS spectrum of the enzymatically generated L-*allo*-Ile.

A

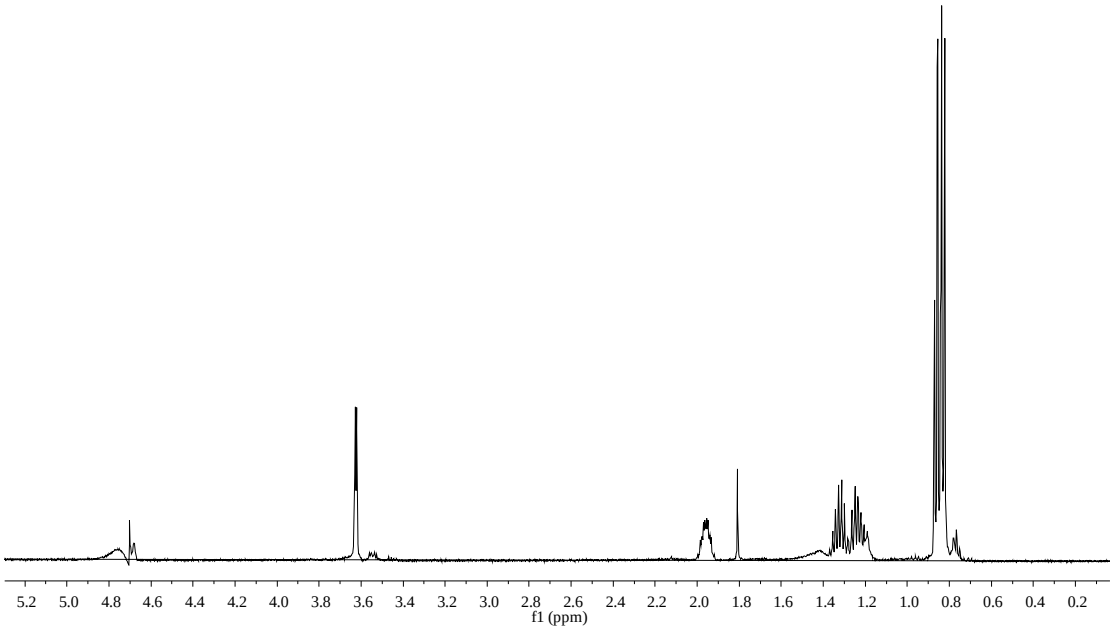

B

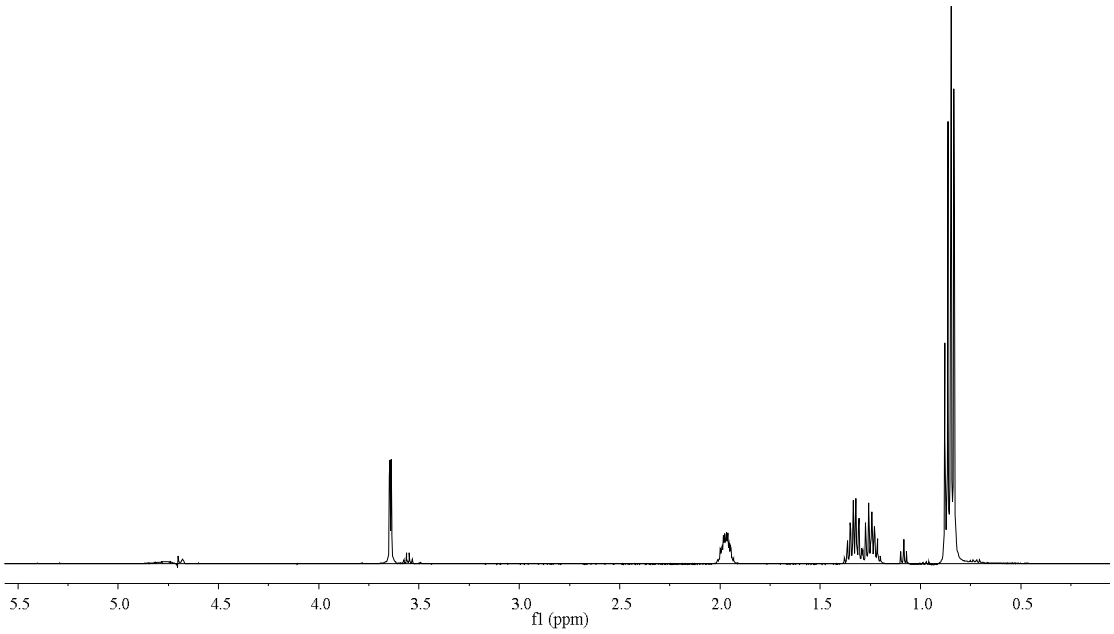

Figure S18. ^{1}H NMR spectra for (A) the enzymatically produced L-*allo*-Ile and (B) the authentic sample of L-*allo*-Ile.

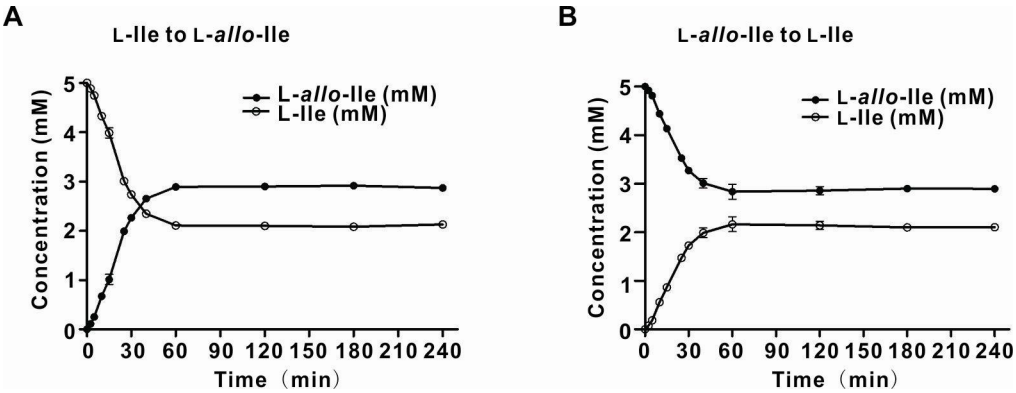

Figure S19. Determination of the equilibrium constant (*K*eq) for DsaD/DsaE-catalyzed bidirectional reaction with (A) L-Ile or (B) L-*allo*-Ile as substrates. Enzyme assays were performed in 50 µL sodium phosphate buffer (50 mM, pH8.0) containing 2.5 µM DsaD, 2.5 µM DsaE, 0.1 mM PLP and 5 mM L-Ile or L-*allo*-Ile as substrate at 30°C in triplicate. Reactions were stopped by addition of 150 µL of methanol after 2.5, 5, 10, 15, 25, 30, 40, 60, 120, 180, 240 min. The *K*eq was calculated using the equation *K*eq = ([product]/[substrate]) at reaction equilibrium. Thus, *K*eq for the reaction with L-Ile as the substrate is 1.37 (*K*eq = ([L-*allo*-Ile]/[L-Ile]) = (2.89/2.11) = 1.37).

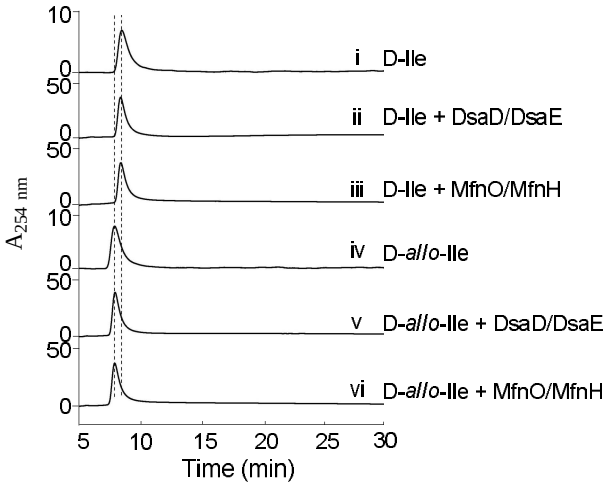

Figure S20. Substrate specificity assays for DsaD/DsaE and MfnO/MfnH. Co-incubation of D-Ile with DsaD/DsaE (ii), MfnO/MfnH (iii) yielded no new peaks. Co-incubation of D-*allo*-Ile with DsaD/DsaE (v), MfnO/MfnH (vi) also yielded no new peaks.

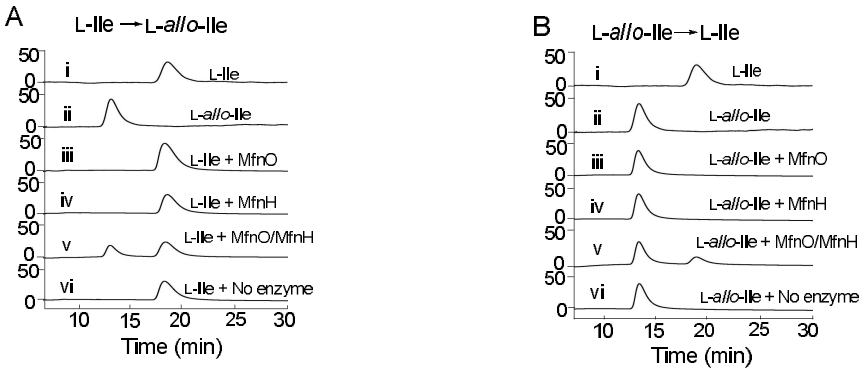

Figure S21. *In vitro* characterization of MfnO/MfnH. (A) Production of L-*allo*-Ile proceeds only upon co-incubation of L-Ile with MfnO and MfnH (v). Enzyme assays with MfnO alone (iii), MfnH alone (iv), or control lacking MfnO/MfnH (vi) yielded only starting substrate L-Ile. (B) Production of L-Ile occurs only upon co-incubation of L-*allo*-Ile with MfnO and MfnH (v). Enzyme assays with MfnO alone (iii), MfnH alone (iv), or control lacking MfnO/MfnH (vi) afforded only starting substrate L-*allo*-Ile.

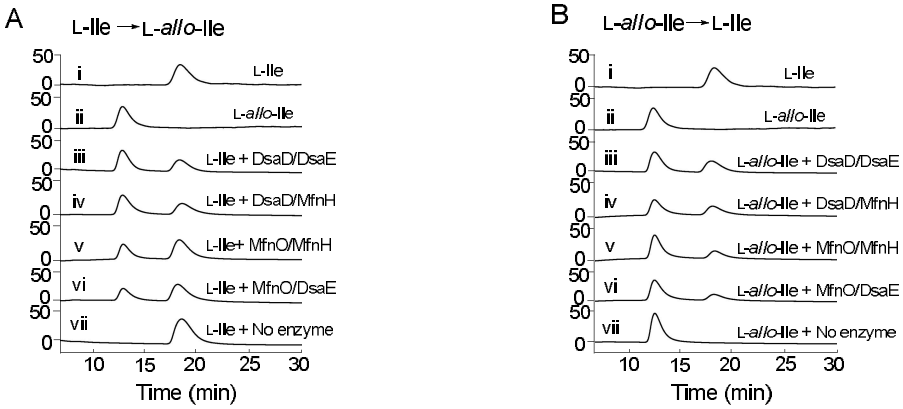

Figure S22. (A) The activity assays of the crossed enzyme pairs DsaD/MfnH and MfnO/DsaE using L-Ile as the substrate. L-*allo*-Ile was generated upon co-incubation with L-Ile and DsaD/DsaE (iii), DsaD/MfnH (iv), MfnO/MfnH (v) and MfnO/DsaE (vi). Control reaction lacking the enzymes failed to afford of L-*allo*-Ile (vii). (B) The activity assays of the crossed enzyme pairs DsaD/MfnH and MfnO/DsaE using L-*allo*-Ile as the substrate. L-Ile was generated upon co-incubation of L-*allo*-Ile with DsaD/DsaE (iii), DsaD/MfnH (iv), MfnO/MfnH (v) and MfnO/DsaE (vi). Control reaction lacking the enzymes failed to afford L-Ile (vii).

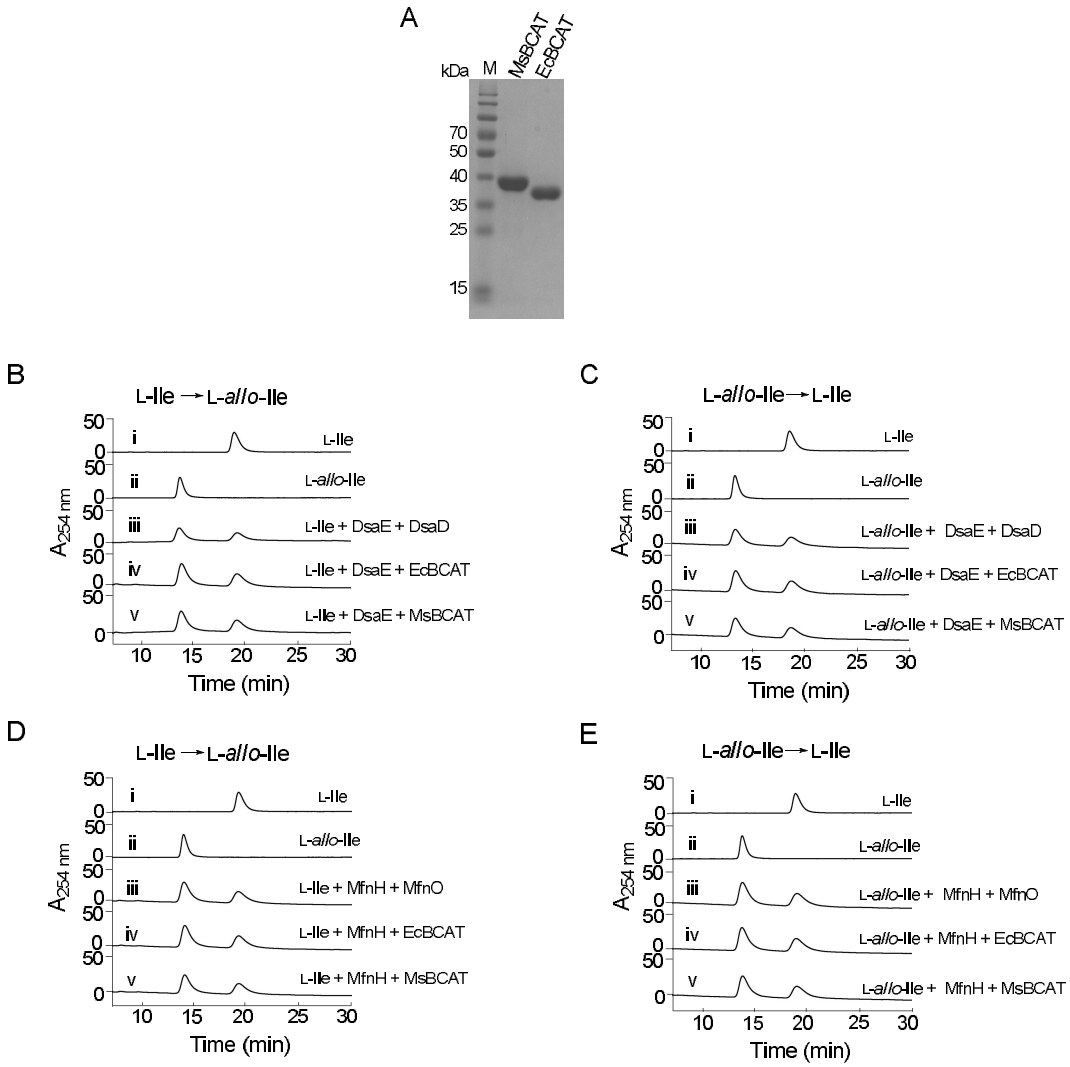

Figurre S23. (A) SDS-PAGE analyses of purified His_6-EcBCAT and His_6-MsBCAT. M: protein markers. (B – E) Activity assays of EcBCAT and MsBCAT from primary metabolism. Co-incubation of EcBCAT or MsBCAT with isomerase DsaE or MfnH using either L-Ile or L-*allo*-Ile as substrates under the standard conditions afforded the respective products L-*allo*-Ile or L-Ile.

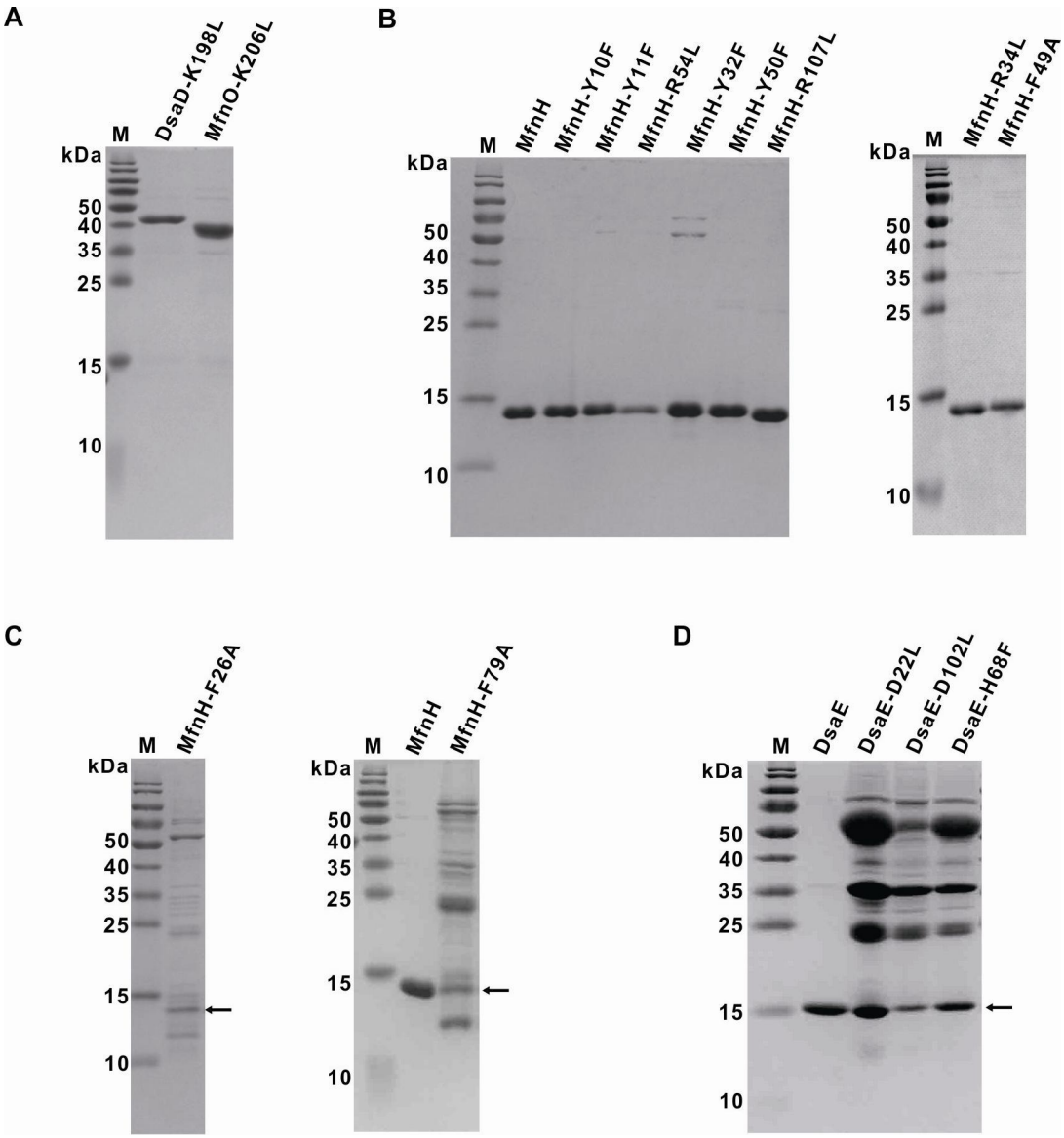

Figure S24. SDS-PAGE analyses of the purified *E. coli*-derived mutants of DsaD, MfnO, MfnH, and DsaE. (A) SDS-PAGE analyses of the aminotransferase DsaD/MfnO mutants. (B) SDS-PAGE analyses of the eight MfnH mutants purified to homogeneity as soluble proteins. (C) SDS-PAGE analyses of the two partially purified MfnH mutants. (D) SDS-PAGE analyses of the three partially purified DsaE mutants. M: protein marker.

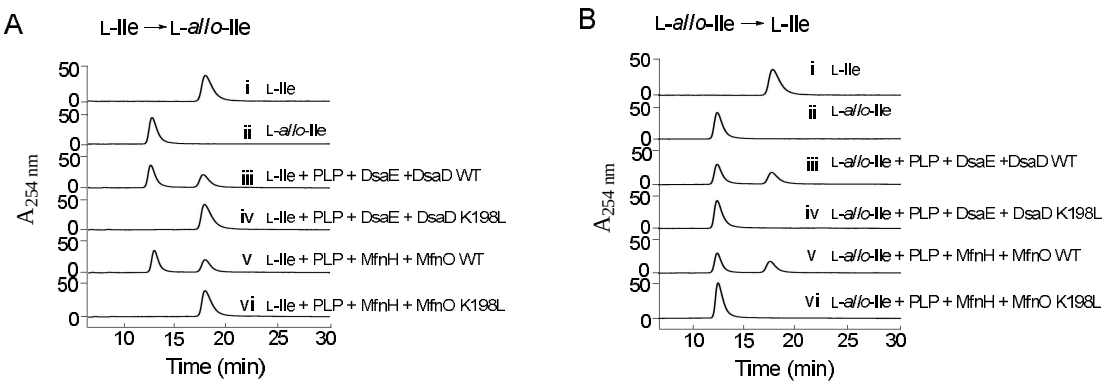

Figure S25. Effect of PLP supplementation upon the DsaD/MfnO mutant enzyme activities. Addition of supplemental PLP to the enzyme reaction mixtures failed to restore DsaD or MfnO enzymatic activities when using (A) L-Ile or (B) L-*allo*-Ile as substrates.

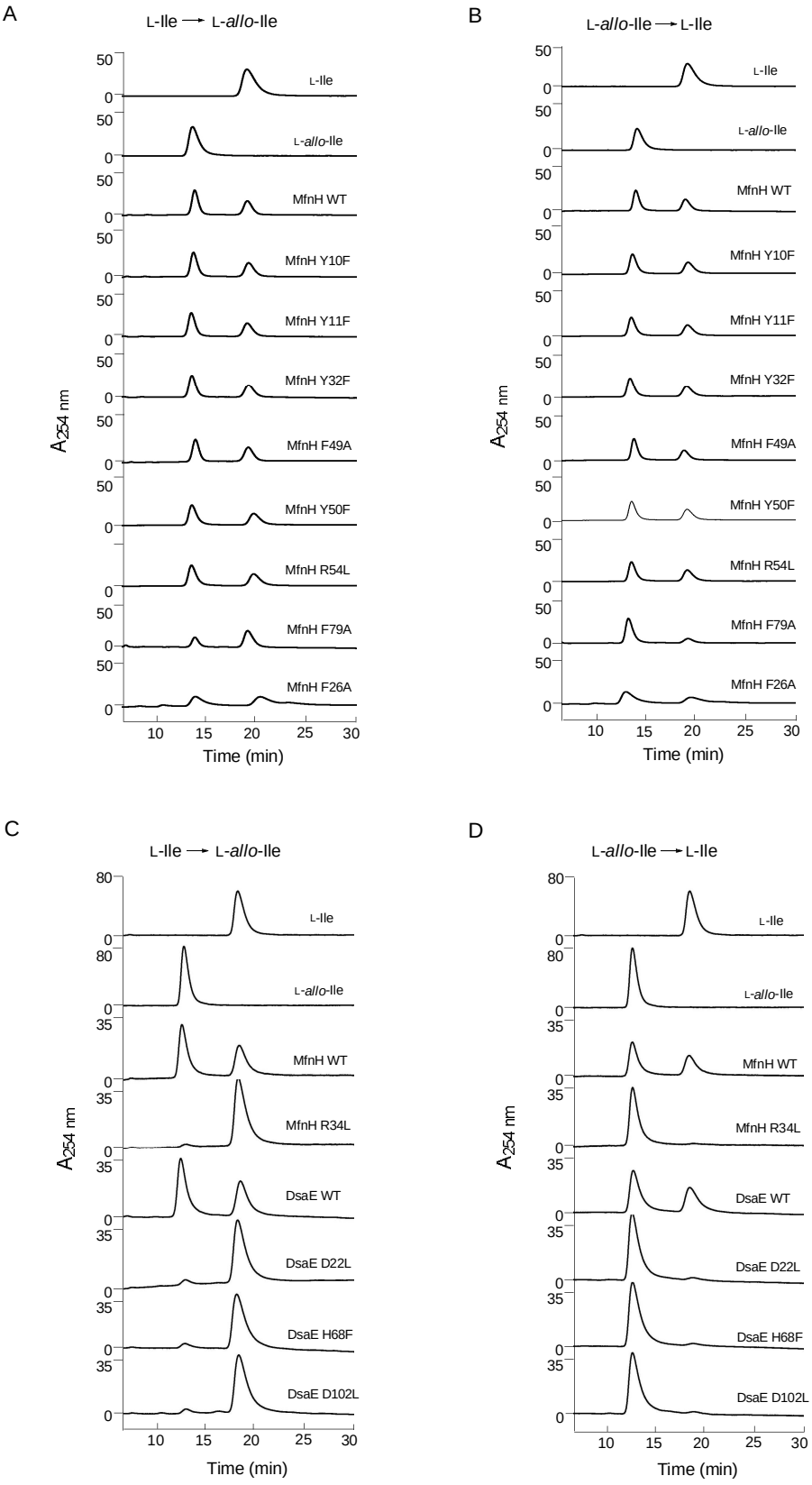
A
L-Ile → L-allo-Ile
L-Ile
L-allo-Ile
MfnH WT
MfnH Y10F
MfnH Y11F
MfnH Y32F
MfnH F49A
MfnH Y50F
MfnH R54L
MfnH F79A
MfnH F26A
A254 nm
Time (min)
B
L-allo-Ile → L-Ile
C
L-Ile → L-allo-Ile
MfnH R34L
DsaE WT
DsaE D22L
DsaE H68F
DsaE D102L
D
L-allo-Ile → L-Ile

Figure S26. HPLC profiles of the activity assays of the eight MfnH mutants as coupled with MfnO using either (A) L-Ile or (B) L-*allo*-Ile as substrates. These eight MfnH mutants displayed no obvious deviations in enzymatic activity relative to wild-type enzyme. Also shown are HPLC profiles of the activity assays of the four MfnH/DsaE mutants as coupled with MfnO or DsaD using (C) L-Ile or (D) L-*allo*-Ile as substrates. These four MfnH/DsaE mutants displayed sharply diminished enzymatic activity corresponding to ~ 8% of that displayed by wild-type MfnH/DsaE.

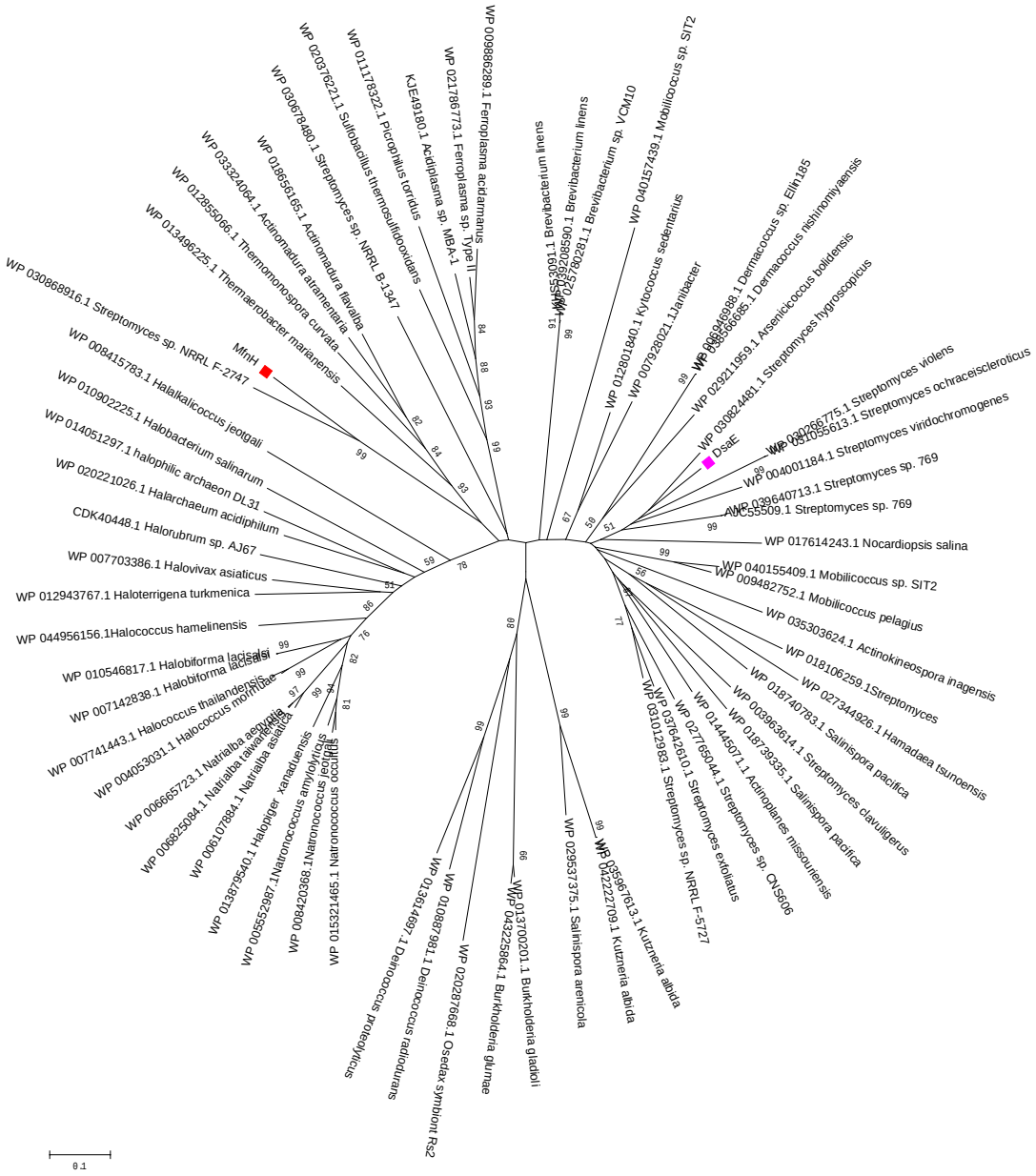

Figure S27. Phylogenetic tree of DsaE/MfnH with their homologues. The amino acid sequences were aligned using ClustalX (2.1) and the phylogenetic tree was generated using Molecular Evolutionary Genetics Analysis (MEGA) 6.0.